Comparison of Pose Estimation Methods of a 3D Laser Tracking System Using Triangulation and Photogrammetry Techniques

Blais, François; Beraldin, Jean-Angelo; El-Hakim, Sabry; Cournoyer, Luc

National Research Council Canada
Conseil national de recherches Canada

Institute for Information Technology
Institut de Technologie de l'information

NRC·CNRC

*Comparison of Pose Estimation Methods for a 3D Laser Tracking System using Triangulation and Programmetry Techniques**

F. Blais, J.-A. Beraldin, S. El-Hakim, and L. Cournoyer
January 2001

***published in** SPIE Proceedings, Electronic Imaging 2001, Videometrics and Optical Methods for 3D Shape Measurement VII, San Jose, CA. January 21–26, 2001. Vol. 4309. NRC 44152.

Comparison of Pose Estimation Methods of a 3D Laser Tracking System using Triangulation and Protogrammetry Techniques [*]

F. Blais[1], J.-A.Beraldin, S. El-Hakim, L. Cournoyer
National Research Council of Canada
Institute for Information Technology
Ottawa, Ontario, Canada, K1A-0R6

ABSTRACT

In this paper, we compare the accuracy and resolution of a 3D-laser scanner prototype that tracks in real-time and computes the relative pose of objects in a 3D space. This 3D-laser scanner prototype was specifically developed to study the use of such a sensor for space applications. The main objective of this project is to provide a robust sensor to assist in the assembly of the International Space Station where high tolerance to ambient illumination is paramount. The laser scanner uses triangulation based range data and photogrammetry methods (spatial resection), to calculate the relative pose of objects. Range information is used to increase the accuracy of the sensing system and to remove erroneous measurements. Two high-speed galvanometers and a collimated laser beam address individual targets mounted on an object to a resolution corresponding to an equivalent imager of 10000×10000 pixels. Knowing the position coordinates of predefined targets on the objects, their relative poses can be computed using either the scanner calibrated 3D coordinates or spatial resection methods.

Keywords: Laser scanner, 3D, ranging, tracking, light immunity, photogrammetry, spatial resection, triangulation.

1. INTRODUCTION

It is widely acknowledged that vision is a key element for space applications and a very crucial component for several key scientific and engineering missions. From the Hubble telescope, to documentation, remote operations, assembly and maintenance of the new International Space Station, vision plays a major role and in many aspects, becoming so important that substitutes cannot be found. Conventional video and still cameras are attractive because of their ease of use, low maintenance, and simplicity of integration to existing equipment. Unfortunately, the presence of the sun or any other strong sources of light adversely affect the quality of video images. Poor contrast between features on the object and background often makes the images difficult to analyse. Even under supervised operation and careful planning by the crew, the wide dynamic range of illumination in orbit is a challenging problem. As an example, the quality of the image of Figure 1 (although visually very impressive) is problematic for automated operation because of lost of details in the object structure and earth background. For example, the existing Space Vision System developed by Neptec Design Group of Ottawa [1] uses the targets on the International Space Station to compute the pose (6 DOF) of the different sections of the station for part alignment during assembly. Missing or distorted targets will adversely affect the performances of the system.

It is therefore desirable to offer a complementary vision system to on-board video cameras that will not be restricted by operational conditions such as sun illumination that produces interference. A range laser scanner approach offers the potential of being 100% operational throughout the changing illumination conditions in orbit (pending tests onboard the space shuttle scheduled for next year). The presence of the sun or any other strong sources of light adversely affect the quality of the conventional methods that rely on standard video images, e.g. closed circuit camera on-board the shuttle. Poor contrast between features on the object, camera saturation, insufficient light and shadows are very serious problems that limit the

[*] NRC-44152
[1] francois.blais@nrc.ca

normal operation of conventional video-based vision systems. Another very important case for automated machine vision system is concerned with lighting gradients (cast shadows), which requires both extended dynamic range for the video camera and sophisticated image processing algorithms. Although this seems a-priori a straightforward problem for the human eye, it is not as simple for limited dynamic range vision systems. It is therefore very important that any complementary systems like a laser scanner be robust to operational conditions such as sun interference, saturation, shadows, or simply insufficient light.

Key to the design of an electro-optical system is the overall application [3]. Although there is a desire for a single electro-optical imaging system to perform all functions, this is still far from being the case. As systems complexity increases and technology advances, more and more functions can be accomplished using a single system, such as this laser scanner. It is also increasingly necessary to define performance requirements for each subsystem to insure that the overall system requirements are met. The laser scanner used for these demonstrations has two high-speed galvanometers and a collimated eye-safe laser beam to address individual targets on the object. High resolution images and excellent tracking accuracy are obtained. References [4,5] details the laser scanner operations and the integration of the laser scanner system with the current Space Vision System for tracking operation.

Figure 1: Example of the effect of sun illumination and earth albedo on video images. The Space Vision System [1,6] uses the known location of the B/W targets to compute the pose of the object(s). Even if this picture is of excellent quality, high contrast between illuminated and dark regions, and shadows are very problematic for automated space vision.

Table 1: Conditions for ambient illumination and their effect on the Laser Scanner System.

Illumination conditions	**Possible effect on laser scanner**
Normal conditions	None – normal conditions
Partial target shadowing	None – outside instantaneous field of view of camera
Full target shadowing	Reduced accuracy – Distortion on signal or saturation
Saturation (Field of view)	Minimal – normally outside instantaneous FOV of camera
No Light (Dark)	None - Ideal for laser scanner

Estimated percentage of "conditions" of operation in orbit

60%	Normal conditions	35%	Shadow conditions
<5%	Saturation & poor illumination	<1%	Back illumination

Our laser-based range scanner approach [7,8,9] offers the advantage of being close to 100% operational throughout the changing illumination conditions in orbit. The laser scanner uses two principal modes of operation: imaging and target tracking. In tracking mode, one of the unique features of this laser scanner is its potential to combine in a single unit different ranging and object pose estimation methods. In this paper we will concentrate on two methods:

- 3D pose estimation, using triangulation and the calibrated XYZ raw coordinates of the targets.
- Spatial resection compatible with current Space Vision System (SVS) used by NASA (photogrammetry techniques).

2. LASER TRACKING SYSTEM

The variable resolution laser scanner of Figure 2 tracks in real time targets and/or geometrical features of an object as shown in Figures 4 and 5. The scanner uses two high-speed galvanometers and a collimated laser beam (Figure 3). Different laser wavelength have been tested, from eye-safe wavelength of 1.5 μm with higher MPE, infrared at 820 nm, and green at 532 nm, with minor modifications to the electro-optics, interference filters, and coatings of the mirrors, lens and windows. The laser scanner addresses individual targets on the object as shown in Figure 5. Very high resolution and excellent tracking accuracy are obtained using Lissajous scanning patterns [7,8]. The method will be described in more detail in section 3.

The small targets visible in Figure 1 (small black dots) are used by the Space Vision System [2,6]. Because the exact locations of these features on the object are known, object position is computed from their relative positions in the video images using a photogrammetry-based technique known as spatial resection. In [4] and in Figure 5, tracking of retro-reflective targets was used to demonstrate the operation of the laser scanner.

The system, with respect to [4,10], can now track conventional Black on White targets as well as retro-reflective targets. For compatibility with current space applications and missions, tracking compatibility with Black Inconel targets was imperative. Tracking B/W targets is a key challenge and system sensitivity becomes a serious issue, reducing the dynamic range of the scanner by more than two orders of magnitude. For sun light immunity, this question becomes mainly a relation between minimum laser signal power reflected back to the laser scanner, relative to the background light as opposed to the minimum signal detected.

Figure 2: Prototype of the laser scanner system. A conventional video camera is "temporarily" mounted on the laser scanner for monitoring and comparison with conventional methods. Dimensions are 27 cm × 18 cm × 10 cm..

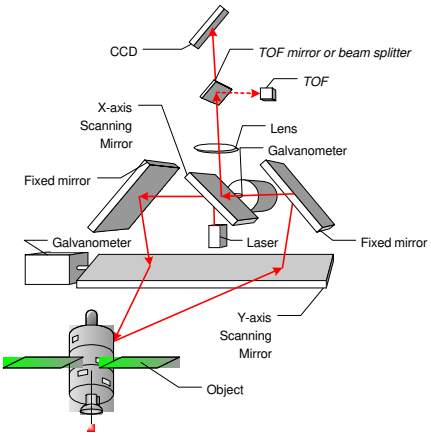

Figure 3: Schematic representation of the auto-synchronized geometry.

In [10] we have analyzed the behavior of this prototype of the laser scanner system and demonstrated the effectiveness of the solution to sun interference. Although it is not as good as retro-reflective targets, we are still obtaining several order of magnitude better SNR than conventional video cameras.

2.1. Range measurement

The laser scanner system can measure range information for each voxel (3-D volumetric element) in the scene. The details of operation of the scanner and the exact mathematical model are available from previous publications where the scanner is operated in imaging mode [5,11,12]. Here, we will use the simplified models illustrated in Figure 6 to model range measurement, using triangulation, and to associate object pose estimation obtained using video camera models shown in Figures 7 and techniques discussed in section 4.

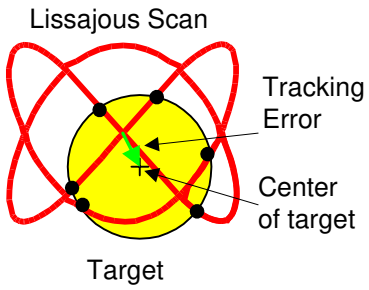

Figure 4: Principle of tracking using the Lissajous pattern and a circular target.

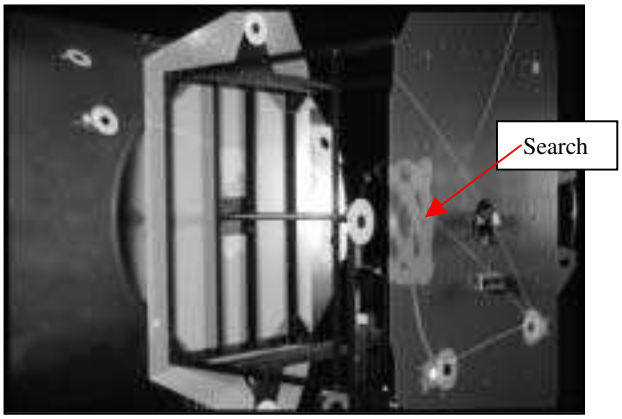

Figure 5: Real-time tracking of targets on the simulated Node and Z1 modules used during the experimentation. Two types of target are visible, Inconel B/W and retro-reflective targets. The system tracks each target sequentially. In this example, one of the targets is in "search mode" (larger Lissajous pattern) while the others are being tracked.

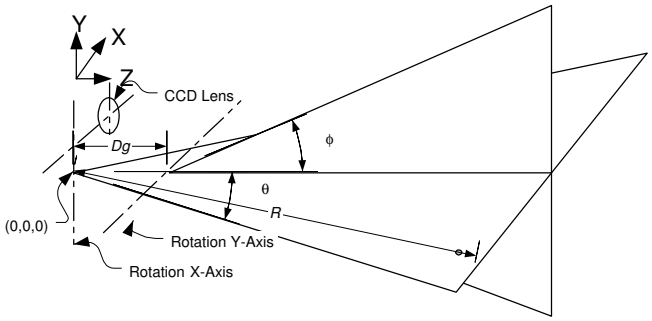

Figure 6: Simplified geometrical model of the laser scanner showing the effect of astigmatism between the X and Y scanning axis.

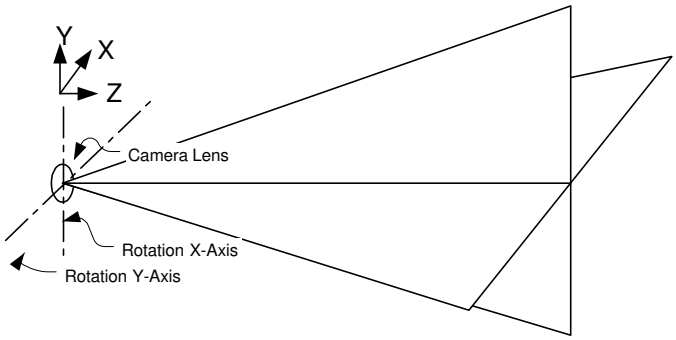

Figure 7: Simplified geometrical model of a simple camera lens system used by conventional camera and photogrammetric methods.

From [11] and from Figure 6, assuming a simplified aberrations-free model and a vergence reduced to 0, setting $R=z/\cos(\theta)$, range R can be calculated as:

$$R = \frac{f \cdot d}{p}\cos(\theta) + d\sin(\theta) \tag{1}$$

where f is the focal length of the lens, d is the triangulation base, θ is the deflection angle following the x-axis, and p is the position of the imaged laser spot of the position sensor (see [8] for details). From Figure 6, the x-y-z coordinates of a point are

$$\begin{bmatrix} x \\ y \\ z \end{bmatrix} = R \cdot \begin{bmatrix} \sin(\theta) \\ (\cos(\theta) - \psi)\sin(\phi) \\ (1-\cos(\phi))\psi + \cos(\theta)\cos(\phi) \end{bmatrix} \tag{2}$$

where θ and ϕ are the deflection angles, and $\psi=Dg/R$ where Dg is the separation between the two scanning mirrors (or axis). Because $Dg<<R$, (operating range R>3m), error propagation calculations (in triangulation mode) can be approximated by

$$\Delta R_{Trian} \approx \frac{R^2}{f \cdot d}\Delta p \tag{3}$$

$$\begin{bmatrix} \Delta x \\ \Delta y \\ \Delta z \end{bmatrix}^2 = \begin{bmatrix} \sin(\theta) \\ \cos(\theta)\cdot\sin(\phi) \\ \cos(\theta)\cos(\phi) \end{bmatrix}^2 \left(\frac{R^2}{f \cdot d}\Delta p\right)^2 + \begin{bmatrix} \cos(\theta) \\ -\sin(\theta)\cdot\sin(\phi) \\ -\sin(\theta)\cos(\phi) \end{bmatrix}^2 R^2 \cdot \Delta\theta^2 + \begin{bmatrix} 0 \\ \cos(\phi) \\ -\sin(\phi) \end{bmatrix}^2 R^2 \cdot \cos^2(\theta) \cdot \Delta\phi^2 \tag{4}$$

where Δp is the uncertainty associated with the laser spot measurement on the CCD of Figure 3.

Figure 8 shows range error measured with the scanner in triangulation (notice the R^2 dependence of the error). Other typical system parameters for the prototype used here are maximum deflection angles of 0.5 rad (30 deg) and angular errors of 50-100 μrad, for 3-cm diameter retro-reflective targets (see section 5). From equation 4 the total system error, for medium to long range, is mostly contributed by range error measurement *ΔR, i.e., Δp* the uncertainty associated with the laser spot measurement.

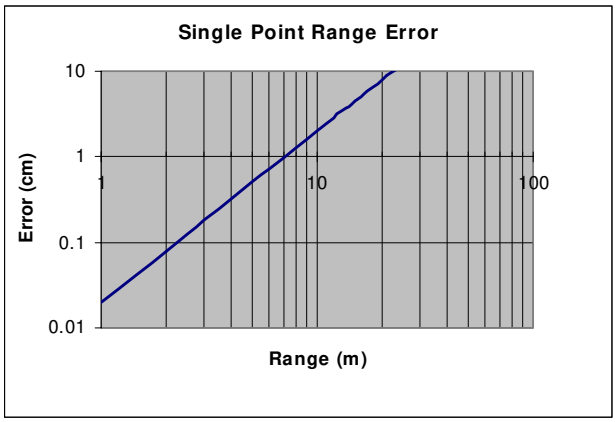

Figure 8: Single point range error accuracy of the Laser Scanner System.

3. REAL-TIME TRACKING – LISSAJOU PATTERNS

Real-time tracking of targets or geometrical features on an object is implemented using Lissajous figures, to obtain good scanning speed and accuracy. Driving the two axis galvanometers with sine waves of different frequency creates a Lissajous pattern [7,8]. The geometrical tracking principle uses both the 3-D range and intensity information on the Lissajous pattern to (a) identify targets on the object or any useful geometrical feature, and (b) to discriminate the target from its background.

Lissajous patterns are used to efficiently scan objects at refresh rates exceeding the bandwidth of the mechanical deflection system. The Lissajous tracking pattern is a key feature to increase angular accuracy used during photogrammetric mode of operation of the scanner.

Figure 4 and 5 illustrate the principle associated with position tracking of targets using a 3:2 Lissajous pattern. Range and intensity data are measured for each of the N points on the scanning pattern. The Lissajous tracking pattern plays a major role in system resolution (and accuracy). In practice, the laser scanner angular resolution is limited mostly by two parameters: sub-pixel resolution and size of the target, and galvanometer mechanical resolution and stability (wobble and jitter) over temperature.

Figure 5 shows the multiple targets tracking process. The laser scanner is programmed to sequentially scan different sections of the object. One of the targets is here in the search mode and the scanner uses a larger Lissajous pattern to locate it. When found, the scanner automatically switches from the *search* mode to the *track* mode using a smaller Lissajous pattern to increase target centroid accuracy. Errors introduced by the measurement process are always minimized because the scanner automatically centers and optimizes the size of the tracking patterns based on the measured target to object distance, for each target individually. The laser scanner scans sequentially different sections or targets on one or several objects.

Tracking stability and pose estimation were tested on the structures of Figure 9. B/W targets bring very serious challenges for automated target detection and tracking:

- Specular reflections created by the metallic structures and the target themselves
- Poor contrast between the white targets and their black background
- Defects and non-uniformity of the targets surfaces
- Variations in the material reflectivity between targets (retro, B/W, W/B)
- Target incident angles
- Ambient intensity variations and shadows introduced by the Sun
- Material reflectivity at wavelength different than visible light
- Target occlusions

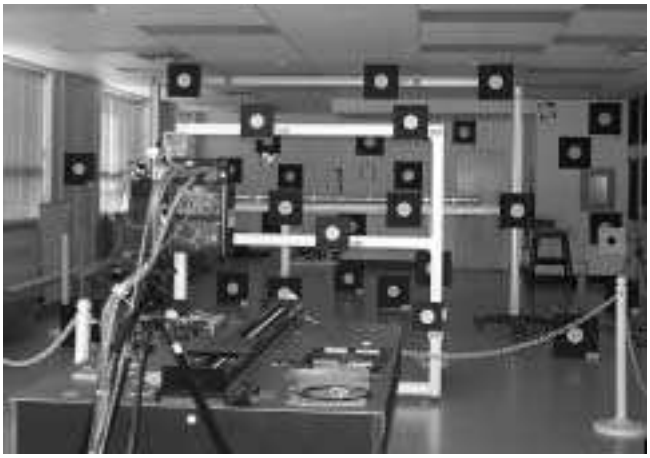

Figure 9: Tracking structure used for pose evaluation. Three groups of targets at different ranges are used to evaluate the performances and stability of the photo-solution.

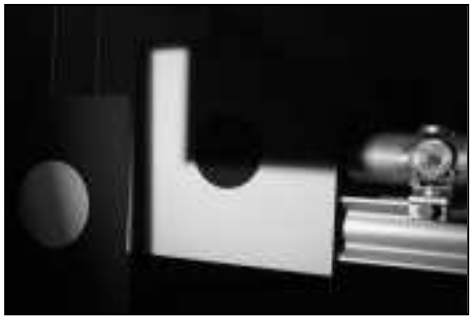

Figure 10: Demonstration of shadow illumination and high intensity contrast created by ambient light.

Although the targets contrast from the video picture appears good, at a wavelength of 820 nm the signal ratio between the white target and its darker background is only 2:1. For the black Inconel target, signal ratio of the target to background is much better (10:1). Other interesting dynamic signal ratios are non-uniform signal response of the “dark” background and sensor vignetting (3:1), variations of reflectivity versus surface incident angle (4:1), specularity of non-diffusing surfaces

(>20:1), ambient light and shadows (3:1), variation of target reflectivity as the square of the distance (>100:1). The laser scanner must exhibits an equivalent SNR of more than 10^4 to 10^5 of dynamic range. This is accomplished by dynamically varying the laser power and the sensitivity of the CCD, used for laser spot measurement, on a per target basis.

Figure 10 shows the effects of sun illumination and shadows on the laser tracking system. In both Figures 9 and 10, the laser light is not seen by the video camera, completely washed out by the brighter ambient light. The tracking effects of Figure 5 were created using long exposure photography.

The locations of the centroid of the detected targets are used to compute the absolute or relative poses (position and orientation) of multiple objects.

4. OBJECT POSE EVALUATION

Object pose evaluation is a complex subject by itself and an in depth mathematical analysis is beyond the scope of this paper. We will rather provide here a qualitative analysis of the method from an empirical point of view. Assuming a set of known coordinates (x_o,y_o,z_o) on a rigid object, the expected location of these targets in the laser scanner 3-D space $(\hat{x},\hat{y},\hat{z})$ is given using homogenous coordinates by:

$$\hat{\mathbf{X}} = \mathbf{M} \cdot \mathbf{X}_o \tag{5}$$

$$\mathbf{X}_o = \begin{bmatrix} x_o & y_o & z_o & 1 \end{bmatrix}^T \tag{6}$$

$$\hat{\mathbf{X}} = \begin{bmatrix} \hat{x} & \hat{y} & \hat{z} & 1 \end{bmatrix}^T \tag{7}$$

where **M** is a 4x4 rigid transformation matrix (|**M**|=1) that maps the object target coordinates in the laser scanner space. The matrix **M** has 6 unknowns, 3 translations and 3 rotations (yaw-pitch-roll). Object pose estimation consists of evaluating the transformation matrix that will minimize a set of error equations. The most commonly used method minimize the quadratic error between the expected position computed from the previous equation and the laser scanner measurements *x-y-z*:

$$\min\left(\sum \mathbf{E}^{\mathbf{T}} \cdot \mathbf{E}\right) \tag{8}$$

$$\mathbf{E} = \mathbf{X} - \hat{\mathbf{X}} \tag{9}$$

$$\mathbf{X} = \begin{bmatrix} x & y & z & 1 \end{bmatrix}^T \tag{10}$$

Different techniques are available to minimize this set of equations such as based on least-squares adjustment, and quaternions. From equation 4 and considering medium to long range applications, the error vector **E** is highly dependent on the range measurement, *R,*

$$\Delta\mathbf{E} \approx R^2 \Delta p \tag{11}$$

Using the basic lens model of Figure 7 and equation 2, and photogrammetry methods, the collinearity equations are given by

$$\begin{bmatrix} u \\ v \end{bmatrix} = \begin{bmatrix} x/z \\ y/z \end{bmatrix} = \begin{bmatrix} \dfrac{\sin(\theta)}{(1-\cos(\phi))\psi + \cos(\theta)\cos(\phi)} \\ \dfrac{(\cos(\theta) - \psi)\sin(\phi)}{(1-\cos(\phi))\psi + \cos(\theta)\cos(\phi)} \end{bmatrix} \tag{12}$$

and pose estimation requires the minimization of the error vector

$$\mathbf{E} = \mathbf{U} - \hat{\mathbf{U}} \tag{13}$$

of the projected vector $\mathbf{U}=[u\ v]^T$. From equation (12), dependence of the error vector **E** on range R is much reduced (only ψ *is a factor of* R). Accuracy of the photogrammetric method should be better than direct range data minimization for medium to long range R. Figure 11 and 12 illustrate the two concepts.

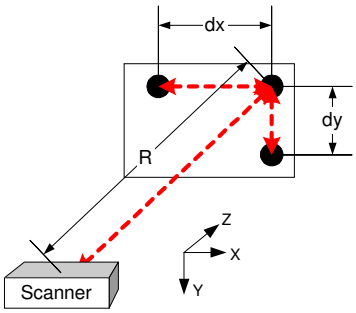

Figure 11: Object pose calculation based on 3D range data.

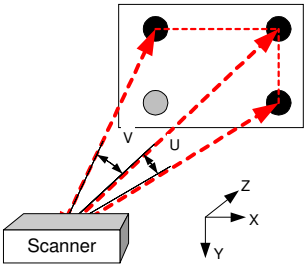

Figure 12: Object pose calculation based on photogrammetry techniques.

5. EXPERIMENTAL RESULTS

Figure 13 shows the results of the model simulation using the previous methods for an 1 m × 1 m array of four 3-cm diameter retro-targets. Increased accuracy using the photogrammetric model UV, compared to XYZ data is important. Furthermore, accuracy varies linearly with range R for the UV method and approximately as $R^{1.5}$ for the XYZ method (triangulation based).

The targets on the structure shown in Figure 9 were divided in three groups and the targets acquired over a period of one hour. Of the 34 targets on the structure, 4 were not used, being occluded by sections of the structure and therefore not visible from the scanner. Standard deviation of the pointing stability for the targets was 130 µrad for the x-axis and 150 µrad for the y-axis. This is not as good as the previous retro-target stability measurement of 80 urad in [10]. This is mainly because the B/W targets are physically much bigger, varying in diameter from 10 cm at 5 m, 20 cm at 9 m, and 20 cm at 17 m.

The poses of the whole structure and each of the three sub-sections were computed. At the time of writing, calibration of the scanner was not fully integrated within the scanner and therefore the data plotted on Figure 13 represents only the stability of the solution over time. Temperature stability also needs to be accessed.

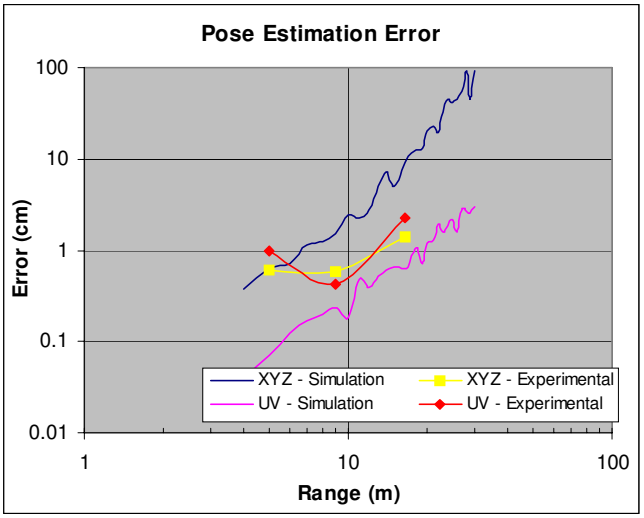

Figure 13: Results of model simulation and experimental results for pose evaluation of rigid transformation matrix

There are three main key factors that must be considered when comparing the simulated data and the experimental results:

- the model uses a regular target array of 1 m $\times$ 1 m, while the experimental data uses targets relatively randomly distributed within the FOV of the laser scanner,
- the B/W targets are bigger than the retro-targets used with the simulation, pointing accuracy is lower and this will directly affect the UV method,
- the B/W targets being bigger (relative to the projected laser beam), this will reduce the noise measurement associated with range (mostly laser speckle) and therefore this will benefit the XYZ method.

From the simulated model, an increased in accuracy using resection is obvious for a given target size and object size. However when targets with different sizes are used, this gain is not as clearly defined. The ranging errors of equation 11 changes because of non-constant laser peak position error Δp. Nevertheless, the experimental results of Figure 13 and the predicted values are consistent and within the boundary limits.

This also clearly demonstrates the advantages of the combined methods, i.e. the use of a laser range scanner as a projective camera.

6. CONCLUSION

A 3-D laser scanner system was presented in this paper that demonstrates excellent tracking characteristics for space assembly operations and high immunity to ambient illumination and sun interference. It uses two high-speed galvanometers and a collimated laser beam to address individual targets on an object. Three types of targets have been tracked in real-time using Lissajous scanning patterns: 1) Retro-reflective targets, 2) White on black background, and 3) Black on white background. In the case of B/W targets, tracking with a SNR of 2:1 on the target returned signal, several order of magnitudes weaker than the surrounding structures and ambient illumination was presented.

Based on the high-resolution pointing measurement and range information for each individual target, the estimation of the 3D poses of objects was computed. Combining the ranging with the high pointing accuracy obtained using the Lissajous tracking pattern, and photogrammetric methods (spatial resection), increased accuracy in the pose estimation of the object, by approximately an order of magnitude, was obtained. This combination of ranging techniques makes the laser scanner compatible with the current Space Vision System (SVS) used by NASA. Experimental range stability of 4 mm was obtained for an object at a distance of 15 m from the camera.

7. REFERENCES

1. www.neptec.com
2. S.G. MacLean, and H.F.L. Pinkney, ``Machine Vision in Space,'' Canadian Aeronautics and Space Journal, 39(2), 63-77 (1993).
3. G.C. Holst, "Electro-Optical Imaging System Performance," SPIE Optical Engineering Press, JCD Publishing, Winter Park, FL., 1995.
4. F.Blais, J.-A. Beraldin, L.Cournoyer, I. Christie, R. Serafini, K. Mason, S. McCarthy, C. Goodall, "Integration of a Tracking Laser Range Camera with the Photogrammetry based Space Vision System", Acquisition, Tracking, and Pointing XIV, Proceedings of SPIE's Aerosense 2000 Vol. 4025, p. 219-228, (2000), Orlando, FL.
5. Beraldin, J.-A., Blais, F., Rioux, M., Cournoyer, L., Laurin, D., and MacLean, S.G. "Eye-safe digital 3D sensing for space applications". Opt. Eng. 39(1): 196-211; Jan. 2000.
6. S.G. MacLean, M. Rioux, F. Blais, J. Grodski, P. Milgram, H.F.L. Pinkney, and B.A. Aikenhead, "Vision System Development in a Space Simulation Laboratory,"in Close-Range Photogrammetry Meets Machine Vision, Proc. Soc. Photo-Opt. Instrum. Eng., 1394, 8-15 (1990).
7. F. Blais, J.-A. Beraldin, M. Rioux, R.A. Couvillon, and S.G. MacLean, "Development of a Real-time Tracking Laser Range Scanner for Space Application," Proceedings Workshop on Computer Vision for Space Applications, Antibes, France, September 22-24, 161-171 (1993).

8. F. Blais, M. Rioux, and S.G. MacLean, “Intelligent, Variable Resolution Laser Scanner for the Space Vision System,” in Acquisition, Tracking, and Pointing V, Proc. Soc. Photo-Opt. Instrum. Eng., 1482, 473-479 (1991).
9. D.G. Laurin, F. Blais, J.-A. Beraldin, and L. Cournoyer, “An eye-safe Imaging and Tracking laser scanner system for space Applications,” Proc. Soc. Photo-Opt. Instrum. Eng. 2748, 168-177 (1996).
10. F. Blais, J.-A. Beraldin, S. El-Hakim, “Range Error Analysis of an Integrated Time-of-Flight, Triangulation, and Photogrammetric 3D Laser Scanning System,” Laser Radar Technology and Applications V, Proceedings of SPIE’s Aerosense 2000 Vol. 4035, p. 236-247, (2000), Orlando, FL.
11. F. Blais, M. Rioux, and J.-A. Beraldin,”Practical Considerations for a Design of a High Precision 3-D Laser Scanner System,” Proc. Soc. Photo-Opt. Instrum. Eng. 959, 225-246 (1988).
12. J.-A. Beraldin, S.F. El-Hakim, and L. Cournoyer, “Practical Range Camera Calibration,” Proc. Soc. Photo-Opt. Instrum. Eng. 2067, 21-31 (1993).
13. K.J. Gaskik,, “Optical Metrology,” 2nd Ed., John Wiley & Sons, West Sussez, England, 1995.